
The Standard Candle Method for Type II Supernovae and the Hubble Constant

Mario Hamuy

The Observatories of the Carnegie Institution of Washington mhamuy@ociw.edu

The “standard candle method” for Type II plateau supernovae produces a Hubble diagram with a dispersion of 0.3 mag, which implies that this technique can produce distances with a precision of 15%. Using four nearby supernovae with Cepheid distances I find $H_0(V)=75\pm 7$, and $H_0(I)=65\pm 12$.

1 Introduction

Type II supernovae are exploding stars characterized by strong hydrogen spectral lines and their proximity to star forming regions, presumably resulting from the gravitational collapse of the cores of massive stars ($M_{ZAMS} > 8 M_{\odot}$). These objects display great variations in their spectra and lightcurves depending on the properties of their progenitors at the time of core collapse and the density of the medium in which they explode [6]. The plateau subclass (SNe IIP) constitutes a well-defined family which can be distinguished by 1) a characteristic “plateau” lightcurve [1], 2) Balmer lines exhibiting broad P-Cygni profiles, and 3) low radio emission [15]. These SNe are thought to have red supergiant progenitors that do not experience significant mass loss and are able to retain most of their H-rich envelopes before explosion.

Although SNe IIP display a wide range in luminosity, rendering their use as standard candles difficult, Hamuy & Pinto (2002) [5] (HP02) used a sample of 17 SNe II to show that the relative luminosities of these objects can be standardized from a spectroscopic measurement of the SN ejecta velocity. Recently, I confirmed the luminosity-velocity relation [7] (H03) from a sample of 24 SNe IIP. This study showed that the “standard candle method” (SCM) yields a Hubble diagram with a dispersion of 0.3 mag, which implies that SNe IIP can be used to derive extragalactic distances with a precision of 15%. Since the work of H03, Cepheid distances to two SNe IIP have been published, bringing to four the total number of SNe IIP with Cepheid distances. In this paper I use these four objects to improve the calibration of the Hubble diagram, and solve for the value of the Hubble constant.

2 The Luminosity-Velocity Relation

The SCM is based on the luminosity-velocity relation, which permits one to standardize the relative luminosities of SNe IIP. Figure 1 shows the latest version, based on 24 genuine SNe IIP. This plot reveals the well-known fact that SNe IIP encompass a wide range (~ 5 mag) in luminosities. This correlation reflects the fact that while the explosion energy increases, so do the kinetic energy and internal energies. Also plotted in this figure with open circles are the explosion models computed by [9] and [10] for stars with $M_{ZAMS} \geq 8 M_{\odot}$, which reveals a reasonable agreement with observations.

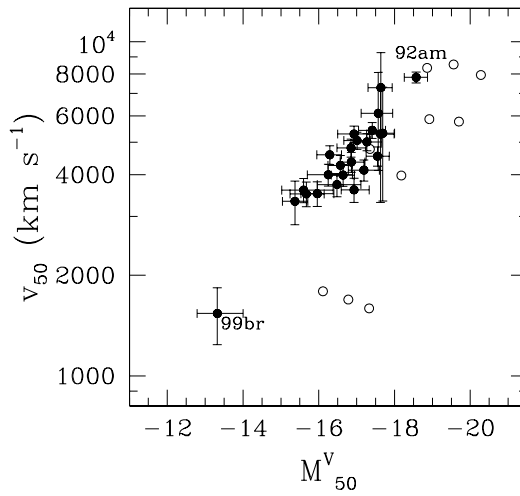


Fig. 1. Envelope velocity versus absolute plateau V magnitude for 24 SNe IIP, both measured in the middle of the plateau (day 50) (filled circles). The expansion velocities were obtained from the minimum of the Fe II $\lambda 5169$ lines. The absolute magnitudes were derived from redshift-based distances and observed magnitudes corrected for dust extinction. Open circles correspond to explosion models computed by [9] and [10] for stars with $M_{ZAMS} \geq 8 M_{\odot}$.

3 The Hubble Diagram

In a uniform and isotropic Universe we expect locally a linear relation between distance and redshift. A perfect standard candle should describe a straight line in the magnitude- $\log(z)$ Hubble diagram, so the observed scatter is a measure of how standard the candle is. Next I assess the performance of the SCM

based on the Hubble diagram constructed with the magnitudes and redshifts given in Table 1 for 24 SNe.

Table 1. Redshifts, Extinction, Magnitudes, and Ejecta Velocities of the 24 Type II Supernovae.

SN	v_{CMB} (km s^{-1}) ± 187	$A_{GAL}(V)$ ± 0.06	$A_{host}(V)$ ± 0.3	V_{50}	I_{50}	v_{50} (km s^{-1})
1968L	321	0.219	0.00	12.03(08)	...	4020(300)
1969L	784	0.205	0.00	13.35(06)	...	4841(300)
1970G	580	0.028	0.00	12.10(15)	...	5041(300)
1973R	808	0.107	1.40	14.56(05)	...	5092(300)
1986I	1333	0.129	0.20	14.55(20)	14.05(09)	3623(300)
1986L	1466	0.099	0.30	14.57(05)	...	4150(300)
1988A	1332	0.136	0.00	15.00(05)	...	4613(300)
1989L	1332	0.123	0.15	15.47(05)	14.54(05)	3529(300)
1990E	1426	0.082	1.45	15.90(20)	14.56(20)	5324(300)
1990K	1818	0.047	0.20	14.50(20)	13.90(05)	6142(2000)
1991al	4484	0.168	0.00	16.62(05)	16.16(05)	7330(2000)
1991G	1152	0.065	0.00	15.53(07)	15.05(09)	3347(500)
1992H	2305	0.054	0.00	14.99(04)	...	5463(300)
1992af	5438	0.171	0.00	17.06(20)	16.56(20)	5322(2000)
1992am	14009	0.164	0.28	18.44(05)	17.99(05)	7868(300)
1992ba	1192	0.193	0.00	15.43(05)	14.76(05)	3523(300)
1993A	8933	0.572	0.05	19.64(05)	18.89(05)	4290(300)
1993S	9649	0.054	0.70	18.96(05)	18.25(05)	4569(300)
1999br	848	0.078	0.65	17.58(05)	16.71(05)	1545(300)
1999ca	3105	0.361	0.68	16.65(05)	15.77(05)	5353(2000)
1999cr	6376	0.324	0.00	18.33(05)	17.63(05)	4389(300)
1999eg	6494	0.388	0.00	18.65(05)	17.94(05)	4012(300)
1999em	838	0.130	0.18	13.98(05)	13.35(05)	3757(300)
1999gi	706	0.055	0.68	14.91(05)	13.98(05)	3617(300)

The CMB redshifts of the SN host galaxies were derived from the observed heliocentric redshifts. For the 16 SNe with $cz < 3000 \text{ km s}^{-1}$ I corrected the redshifts for the peculiar motion of the SN hosts using the parametric model for peculiar flows of [14] (see H03 for details). In all cases I assigned an uncertainty of $\pm 187 \text{ km s}^{-1}$, which corresponds to the cosmic thermal velocity yielded by the parametric model.

A convenient choice for SNe IIP is to use magnitudes in the middle of the plateau, so I interpolated the observed V and I fluxes to the time corresponding to 50 days after explosion. In order to use SNe IIP as standardized candles it proves necessary to correct the observed fluxes for dust absorption. The determination of Galactic extinction is under good control thanks to the IR dust maps of [12], which permit one to estimate $A_{GAL}(V)$ to $\pm 0.06 \text{ mag}$. The

determination of absorption in the host galaxy, on the other hand, is difficult. In H03 I described a method which assumes that SNe IIP should all reach the same color toward the end of the plateau phase. The underlying assumption is that the opacity in SNe IIP is dominated by e^- scattering, so they should all reach the temperature of hydrogen recombination as they evolve [2]. The method is not fully satisfactory since some discrepancies were obtained from $B - V$ and $V - I$ (probably caused by metallicity variations from SN to SN). An uncertainty of ± 0.3 mag can be assigned to this technique based on the reddening difference yielded by both colors.

The ejecta velocities come from the minimum of the Fe II $\lambda 5169$ lines interpolated to day 50, which is good to ± 300 km s $^{-1}$ [4]. In the four cases where I had to extrapolate velocities I adopted an uncertainty of ± 2000 km s $^{-1}$.

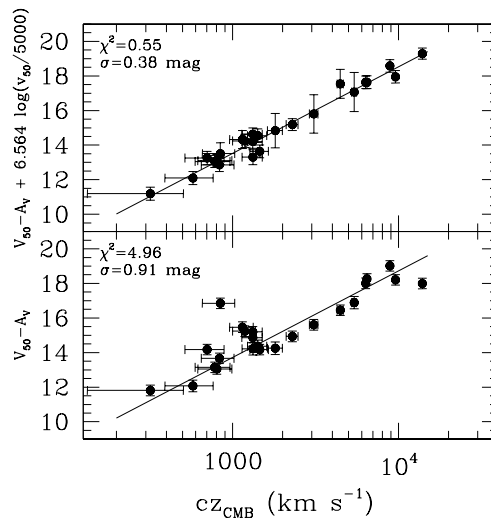


Fig. 2. (bottom) Raw Hubble diagram from SNe II plateau V magnitudes. (top) Hubble diagram from V magnitudes corrected for envelope expansion velocities.

The bottom panel of Fig. 2 shows the Hubble diagram in the V band, after correcting the apparent magnitudes for the reddening values, while the top panel shows the same magnitudes after correction for expansion velocities. A least-squares fit to the data in the top panel yields the following solution,

$$V_{50} - A_V + 6.564(\pm 0.88) \log(v_{50}/5000) = 5 \log(cz) - 1.478(\pm 0.11). \quad (1)$$

The scatter drops from 0.91 mag to 0.38 mag, thus demonstrating that the correction for ejecta velocities standardizes the luminosities of SNe IIP significantly. It is interesting to note that part of the spread comes from the nearby

SNe which are potentially more affected by peculiar motions of their host galaxies. When the sample is restricted to the eight objects with $cz > 3,000$ km s⁻¹, the scatter drops to only 0.33 mag. The corresponding fit for the restricted sample is,

$$V_{50} - A_V + 6.249(\pm 1.35) \log(v_{50}/5000) = 5 \log(cz) - 1.464(\pm 0.15). \quad (2)$$

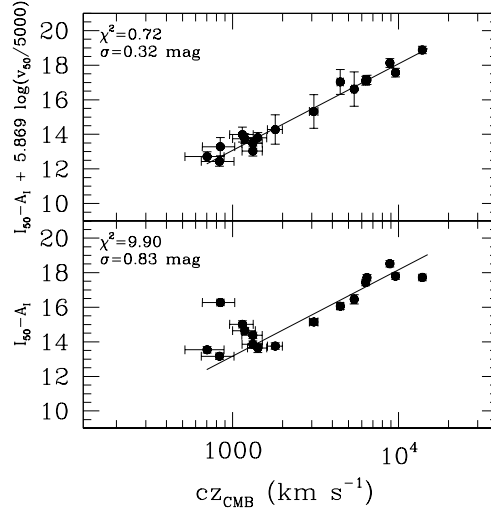


Fig. 3. (bottom) Raw Hubble diagram from SNe II plateau I magnitudes. (top) Hubble diagram from I magnitudes corrected for envelope expansion velocities.

Figure 3 shows the same analysis but in the I band. In this case the scatter in the raw Hubble diagram is 0.83 mag, which drops to 0.32 mag after correction for ejecta velocities. This is even smaller than the 0.38 spread in the V band, possibly due to the fact that the effects of dust extinction are smaller at these wavelengths. The least-squares fit yields the following solution,

$$I_{50} - A_I + 5.869(\pm 0.68) \log(v_{50}/5000) = 5 \log(cz) - 1.926(\pm 0.09). \quad (3)$$

When the eight most distant objects are employed the spread is 0.29 mag, similar to that obtained from the V magnitudes and the same sample, and the solution is,

$$I_{50} - A_I + 5.445(\pm 0.91) \log(v_{50}/5000) = 5 \log(cz) - 1.923(\pm 0.11). \quad (4)$$

4 The Value of the Hubble Constant

The SCM can be used to solve for the Hubble constant, provided the distance to a nearby SN is known. If the distance D of the calibrator is known, and the distant sample is adopted, the Hubble constant is given by

$$H_0(V) = \frac{10^{V_{50} - A_V + 6.249 \log(v_{50}/5000) + 1.464}}{D}, \quad (5)$$

$$H_0(I) = \frac{10^{I_{50} - A_I + 5.445 \log(v_{50}/5000) + 1.923}}{D}. \quad (6)$$

Among the objects of our sample SN 1968L, SN 1970G, SN 1973R, and SN 1999em have precise Cepheid distances. The distances and the corresponding H_0 values are summarized in Table 2. SN 1999em is the only object that provides independent values from the V and I bands, and the results agree remarkably well. Within the uncertainties the values derived from the V -band magnitudes are in good agreement for all four objects, and the average proves to be $H_0(V) = 75 \pm 7 \text{ km s}^{-1} \text{ Mpc}^{-1}$.

Currently, the most precise extragalactic distance indicators are the peak luminosities of SNe Ia. While the HST Key Project yielded a value of $H_0 = 71 \pm 2$ [3], Sandage and collaborators derived $H_0 = 59 \pm 6$ [11]. The difference is mostly due to systematic uncertainties in the Cepheid distances of the calibrating SNe. Since SCM is mainly calibrated with Cepheid distances of the HST Key Project, I conclude that both SNe Ia and SNe IIP give consistent results, which lends further credibility to the SCM.

Table 2. The Hubble Constant.

SN	Distance Modulus	Reference	$H_0(V)$ ($\text{km s}^{-1} \text{ Mpc}^{-1}$)	$H_0(I)$ ($\text{km s}^{-1} \text{ Mpc}^{-1}$)
1968L	28.25(15)	[13]	77 ± 15	...
1970G	29.13(11)	[3]	77 ± 13	...
1973R	29.86(08)	[3]	87 ± 15	...
1999em	30.34(19)	[8]	64 ± 13	65 ± 12
Average			75 ± 7	65 ± 12

HP02 found a value of $H_0 = 55 \pm 12$ based on one calibrator (SN 1987A), which proves significantly lower than the current 65-75 range. The main reason for this difference is that SN 1987A is not a plateau event and should not have been included in the HP02 sample since the physics of its lightcurve is different than that of SNe IIP.

5 Conclusions and Discussion

This sample of 24 SNe IIP shows that the luminosity-velocity relation can be used to standardize the luminosities of these objects. The resulting Hubble diagram has a dispersion of 0.3 mag, which implies that SNe IIP can produce distances with a precision of 15%. Using four nearby SNe with Cepheid distances I find $H_0(V)=75\pm7$ and $H_0(I)=65\pm12$. These values compare with $H_0=71\pm2$ derived from SNe Ia [3], which lends further credibility to the SCM.

This study confirms that SNe IIP offer great potential as distance indicators. The recently launched Carnegie Supernova Program at Las Campanas Observatory has already targeted ~ 20 such SNe and in the next years it will produce an unprecedented database of spectroscopy and photometry for ~ 100 nearby SNe, which will be ideally suited for cosmological studies.

Although the precision of the SCM is only half as good as that produced by SNe Ia, with the 8-m class telescopes currently in operation it should be possible to get spectroscopy of SNe IIP down to $V\sim 23$ and start populating the Hubble diagram up to $z\sim 0.3$. A handful of SNe IIP will allow us to get an independent check on the distances to SNe Ia.

Support for this work was provided by NASA through Hubble Fellowship grant HST-HF-01139.01-A awarded by the Space Telescope Science Institute, which is operated by the Association of Universities for Research in Astronomy, Inc., for NASA, under contract NAS 5-26555.

References

1. R. Barbon, F. Ciatti, L. Rosino: *A&A* **72**, 287 (1979)
2. R.G. Eastman, B.P. Schmidt, R. Kirshner: *ApJ* **466**, 911 (1996)
3. W.L. Freedman et al: *ApJ* **553**, 47 (2001)
4. M. Hamuy: Type II supernovae as distance indicators. Ph.D. Thesis, Univ. Arizona, Tucson (2001)
5. M. Hamuy, P.A. Pinto: *ApJ* **566**, L63 (2002) (HP02)
6. M. Hamuy: Review on the observed and physical properties of core collapse supernovae. In: *Core Collapse of Massive Stars*, ed by C.L. Fryer (Kluwer, Dordrecht 2003a) in press (astro-ph/0301006)
7. M. Hamuy: The latest version of the standardized candle method for type II supernovae. In: *Carnegie Observatories Astrophysics Series*, vol 2, ed by W.L. Freedman (Cambridge, Cambridge Univ. Press 2003b) in press (astro-ph/0301281)
8. D.C. Leonard, S.M. Kanbur, C.C. Ngeow, N.R. Tanvir: *ApJ* , in press (2003) (astro-ph/0305259)
9. I.Y. Litvinova, D.K. Nadezhin: *Ap&SS* **89**, 89 (1983)
10. I.Y. Litvinova, D.K. Nadezhin: *SvAL* **11**, 145 (1985)
11. B.R. Parodi, A. Saha, A. Sandage, G.A. Tammann: *ApJ* **540**, 634 (2000)
12. D.J. Schlegel, D.P. Finkbeiner, M. Davis: *ApJ* **500**, 525 (1998)
13. F. Thim et al: *ApJ* **590**, 256 (2003)
14. J.L. Tonry, J.P. Blakeslee, E.A. Ajhar, A. Dressler: *ApJ* **530**, 625 (2000)
15. K.W. Weiler, N. Panagia, M.J. Montes, R.A. Sramek: *ARA&A* **40**, 387 (2002)